pH-Induced Alteration and Oxidative Destruction of Heme in Purified Chromaffin Granule Cytochrome b_{561}: Implications for the Oxidative Stress in Catecholaminergic Neurons†

Srimevan Wanduragala,‡ D. Shyamali Wimalasena,‡ Donovan C. Haines,‡,§ Pawan K. Kahol,# and Kandatege Wimalasena*,‡

Department of Chemistry and Department of Physics, Wichita State University, Wichita, Kansas 67260-0051

Received November 19, 2002; Revised Manuscript Received January 27, 2003

ABSTRACT: The transmembrane hemoprotein, cytochrome b_{561} (b_{561}), in the neuroendocrine secretory vesicles is shown to shuttle electrons from the cytosolic ascorbate (Asc) to the intravesicular matrix to provide reducing equivalents for the dopamine β-monooxygenase (DβM) reaction. Intravesicular Asc may also play a role in relieving catecholamine-induced oxidative stress in catecholaminergic neurons. In the present study, we have examined the alteration of purified oxidized b_{561} ($b_{561,ox}$) under mild alkaline conditions to probe the structural and functional characteristics of the protein, using UV−vis and EPR spectroscopic and kinetic techniques. Our results show that low spin heme in oxidized b_{561} ($b_{561,ox}$) readily transforms to an altered high spin form and then slowly to an Asc nonreducible form, in a pH-, temperature-, and time-dependent manner, which can be described by single-exponential rate equations, $A_t = A_o(1 - e^{-kt})$ and $A_t = A_o e^{-kt}$, respectively. More than half of the Asc nonreducible altered b_{561} could be converted back to the native b_{561} by pH adjustment followed by dithionite reduction, suggesting the reversibility of the process. The heme center of the transformed Asc nonreducible protein is completely bleached instantaneously by dithionite in the presence of atmospheric oxygen, which appears to be mediated by molecular oxygen and/or hydrogen peroxide. These results demonstrate that the heme centers of the protein are susceptible to the pH-induced alteration and oxidative destruction, raising some questions regarding the proposed one alkaline labile, two-heme model of b_{561} [Tsubaki, M.; Nakayama, M.; Okuyama, E.; Ichikawa, Y. (1997) *J. Biol. Chem. 272,* 23206−23210]. The pH-induced alteration and the destruction of heme under oxidative conditions may play a significant role in the amplification of oxidative stress in catecholaminergic neurons.

Ascorbic acid (Asc)[1] is a stoichiometric reductant for the dopamine β-monooxygenase (DβM)-catalyzed conversion of dopamine (DA) to norepinephrine (NE) in adrenergic and noradrenergic neurons and in chromaffin granules of the adrenal medulla (*1*−*2*). Asc functions as a single-electron donor producing semidehydroascorbic acid as the immediate product during DβM turnover (*3*−*6*). Semidehydroascorbic acid spontaneously disproportionates to produce Asc and dehydroascorbic acid (fully oxidized form) under in vivo conditions. Although dehydroascorbic acid is reduced back to Asc by glutathione in erythrocytes (*7*) and by a glutathione-dependent enzyme system in plants (*8*−*9*), no mechanism is available to regenerate Asc from dehydroascorbic acid, in catecholamine storage vesicles. Since neuroendocrine secretory vesicles of the adrenal medullae or other endocrine glands do not transfer reduced Asc across the vesicle membrane (*10*−*13*) and the fact that the concentration of Asc in the catecholamine secretory vesicles is approximately 20 mM and catecholamine [NE + epinephrine (E)] concentration is about 500 mM (*1*−*2*), the reducing equivalents must be provided from the cytosol to the interior of the granule for the DβM monooxygenation reaction. The transmembrane hemoprotein, cytochrome b_{561} (b_{561}), is shown to shuttle electrons from the cytosolic pool of Asc [1−3 mM, (*14*)] to the intravesicular matrix to regenerate Asc from semidehydroascorbate. According to this model, semidehydroascorbic acid generated within the granule matrix is efficiently reduced by b_{561} at the expense of cytosolic Asc, preventing the radical disproportionation and thereby maintaining a constant pool of Asc within the granule matrix (*15*−*20*). However, our previous studies with resealed chromaffin granule ghosts (*20*) suggest that while extravesicular Asc exclusively provides reducing equivalents for the membrane bound DβM-catalyzed conversion of dopamine to norepinephrine, intravesicular Asc may not directly interact with the enzyme.

† This work was supported by the National Institutes of Health (NS 39423 to K.W.) and by NSF-EPSCoR (OSR-9255223 to P.K.K. to acquire an EPR spectrometer).

* To whom correspondence should be addressed. E-mail: kandatege.wimalasena@wichita.edu. Tel: (316) 978-7386; Fax (316) 978-3431.

‡ Department of Chemistry.

Department of Physics.

§ Current Address: Department of Chemistry, University of Texas at Dallas, Richardson, Texas 75083-0688.

[1] Abbreviations: Asc, ascorbic acid; b_{561}, cytochrome b_{561}; $b_{561,ox}$, $K_3Fe(CN)_6$-oxidized cytochrome b_{561}; DA, dopamine; DβM, dopamine β-monooxygenase; E, epinephrine; EPR, electron paramagnetic resonance; FPLC, fast protein liquid chromatography; NE, norepinephrine; SDS, sodium dodecyl sulfate.

10.1021/bi0206661 CCC: $25.00
Published on Web 03/07/2003

Bovine adrenal chromaffin granule b_{561} has been purified to homogeneity (*21*), cloned, sequenced (*22*), and shown to be a single polypeptide of 27 700 Da (*22*−*23*). It is functionally and structurally distinct from other electron transport proteins such as mitochondrial cytochromes (*21*−*24*) and has a relatively high reduction potential. The reduced protein shows a characteristic UV−vis spectrum with a Soret band at 427 nm, an asymmetric α-band at 561 nm, and a broad β-band at 530 nm (*25*). In contrast to the early proposal that b_{561} contains one b type heme (*21*−*26*), studies of Burbaev et al. (*27*) and Esposti et al. (*28*) have suggested that two spectroscopically distinguishable forms of heme are present in b_{561} of intact chromaffin granule membranes. In agreement with the early model of Esposti et al. (*28*), Tsubaki et al. (*29*) have recently suggested that purified bovine adrenal b_{561} contains two b type hemes which are located in the interior and the cytosolic phase of the granule with histidines as axial ligands. These authors have further shown that while the exterior heme center is reduced by Asc, the interior heme center which is labile under mild alkaline conditions is oxidized by semidehydroascorbate (*30*−*32*). More recently, Kamensky and Palmer have proposed that as much as three spectroscopically distinguishable heme centers are present in the intact bovine chromaffin granule membrane (*33*). Recent labeling studies have revealed that an essential unprotonated histidine residue in the Asc binding site is intimately associated with the reduction of heme in b_{561} (*34*−*36*). However, the detailed structural parameters as well as the molecular mechanism of the transmembrane electron transfer through b_{561} are still poorly understood.

In the present study, we have examined the alteration of purified b_{561} under mild alkaline conditions to provide additional structural and functional information on the heme in b_{561}, using UV−vis and EPR spectroscopic and kinetic techniques. Our results show that low spin heme in oxidized b_{561} ($b_{561,ox}$) readily transforms to an altered high spin form and then slowly to an Asc nonreducible form, in a pH-, temperature-, and time-dependent manner, which can be described by single-exponential rate equations, $A_t = A_o(1 - e^{-kt})$ and $A_t = A_o e^{-kt}$, respectively. More than half of the Asc nonreducible altered b_{561} could be converted back to the native b_{561} by pH adjustment followed by dithionite reduction, suggesting the reversibility of the process. The present experimental data are consistent with a model in which one of the axial histidines of the protein is replaced with a weak ligand such as water under mild alkaline conditions, resulting in the conversion of the low spin heme center(s) to an initial high spin from. The initial high spin form is further transformed into a second high spin form which is Asc nonreducible. The heme center of the Asc nonreducible protein is bleached instantaneously by dithionite in the presence of atmospheric oxygen which appears to be mediated by molecular oxygen and/or hydrogen peroxide. The significance of these findings with respect to the amplification of the inherent oxidative stress in catecholaminergic neurons are discussed.

MATERIALS AND METHODS

Materials. Ascorbic acid (Asc), $K_3Fe(CN)_6$, and sodium dithionite were obtained from Aldrich. Tween-20 and tyramine hydrochloride were from Sigma. Beef liver catalase (65 000 units/mg of protein) and dithiothreitol were from Boehringer-Mannheim. SDS−PAGE reagents were from Bio-Rad and *n*-octyl β-D-glucopyranoside was from Calbiochem. All other chemicals were of the highest purity obtainable. Microcon YM-30 ultrafiltration devices were from Millipore Co, USA.

General Methods. All UV−visible spectrophotometric measurements were carried out on a Varian 300 Bio double beam UV−visible spectrophotometer equipped with a temperature-regulated multicell compartment at 25 °C using 1.00 cm quartz cuvettes. All chromatographic protein separations were carried out on a FPLC system (Pharmacia-LKB) equipped with a diode array detector, at 4 °C. The purity of the protein was estimated by SDS gel electrophoresis. EPR spectra were recorded on a Bruker EMX X-band EPR spectrometer equipped with a liquid helium cryostat. The EPR spectra of oxidized b_{561} were usually recorded at 15 and 4 K at 9.46 GHz using 20 mW power, 100 kHz modulation frequency and a modulation amplitude of 10 G unless otherwise stated.

Purification of Cytochrome b_{561} from n-Octyl β-D-Glucopyranoside Solubilized Membranes. Chromaffin granules from bovine adrenal medulla were prepared as previously described with minor modifications (*37*−*38*). Catalase (100 μg/mL) was included in all the steps to protect membrane proteins from oxidative damage. The granules were subjected to several freeze/thaw cycles to ensure complete lyses. The lysed granules were diluted with 20 mM potassium phosphate buffer, pH 7.0, and centrifuged at 25000*g* for 25 min at 4 °C to isolate the granule membranes.

The membrane fraction was resuspended in 15 mL (for 50 g of wet medulla tissue) of 50 mM potassium phosphate, pH 7.0 containing 100 μg/mL catalase and 20% (w/v) Tween-20 and stirred for 1 h at 4 °C in the dark, under nitrogen. The sample was centrifuged at 202000*g* for 1 h at 4 °C. The supernatant was discarded and the pellets were rinsed with 3 × 1 mL 20 mM potassium phosphate pH 7.0, to remove the remaining Tween-20. The Tween-20 washed pellets were resuspended in 60 mL (for 50 g of wet medulla tissue) of 25 mM diethanolamine·HCl, pH 9.3, containing 1% (w/v) *n*-octyl β-D-glucopyranoside, 0.5 mM dithiothreitol, and 100 μg/mL catalase. The sample was stirred in the dark for 1 h at 4 °C under nitrogen and was centrifuged at 202000*g* for 1 h at 4 °C. The supernatant was loaded onto a Mono-Q column (Pharmacia-LKB HR 10/10; preequilibrated with 25 mM diethanolamine·HCl, pH 9.3, containing 1% (w/v) *n*-octyl β-D-glucopyranoside, 0.5 mM dithiothreitol) controlled by a Pharmacia FPLC system equipped with a Diode Array UV−vis spectrophotometer (Hewlett-Packard) with a flow through cell assembly as a detector, at 4 °C, with a flow rate of 2 mL/min. The column was washed with the equilibration buffer at 2 mL/min until the A_{280} returned to baseline. The b_{561} was eluted at a flow rate of 2 mL/min using a step gradient of NaCl (0−62.5 mM for 5 min, 62.5−150 mM for 100 min, and 150 mM to 500 mM for 10 min) in 25 mM diethanolamine·HCl, pH 9.3, containing 1% *n*-octyl β-D-glucopyranoside, 0.5 mM dithiothreitol. In a typical experiment most of the b_{561} elutes at 75−105 mM NaCl. Fractions with high 427 nm absorbance were combined, concentrated, and reconstituted into the storage buffer containing 20 mM potassium phosphate, pH 6.8, 20% (w/v) glycerol, 1% (w/v) *n*-octyl β-D-glucopyranoside, 0.5 mM dithiothreitol, except when special storage conditions were

necessary for subsequent experiments.

UV−Visible Spectral Characteristics of Oxidized and Reduced Cytochrome b_{561}. All the spectra were recorded in 20 mM potassium phosphate buffer, pH 6.8, 20% (w/v) glycerol, 1% (w/v) *n*-octyl β-D-glucopyranoside. Purified b_{561} was oxidized with a slight excess of $K_3Fe(CN)_6$ in 100 mM potassium phosphate buffer, pH 6.8, 20% (w/v) glycerol, 1% (w/v) *n*-octyl β-D-glucopyranoside. The excess $K_3Fe(CN)_6$ and $K_4Fe(CN)_6$ were removed by ultrafiltration in an Amicon Cell using a YM-30 membrane. The concentrated, oxidized b_{561} was stored at −70 °C in a storage buffer containing 20 mM potassium phosphate buffer, pH 6.8, 20% (w/v) glycerol, 1% (w/v) *n*-octyl β-D-glucopyranoside for the following experiments unless otherwise stated. The spectra were recorded immediately after the reduction of the oxidized b_{561} with 2 mM Asc followed by 5 mM dithionite. The concentration of b_{561} was determined by using an extinction coefficient of 267.9 mM^{-1} cm^{-1} at 427 nm for the dithionite-reduced protein (*29*).

pH-Dependent Alteration of b_{561}. A 50 μL sample of purified, $K_3Fe(CN)_6$-oxidized b_{561} (2.45 μM) in storage buffer was diluted with 300 μL of 100 mM potassium phosphate buffer, pH 8.0, containing, 20% (w/v) glycerol, 1% (w/v) *n*-octyl β-D-glucopyranoside and incubated at 25 °C in the presence or absence of 20 mM tyramine. The spectra of the samples were recorded every 3 min for a period of 66 min against an identical control except that b_{561} was substituted with storage buffer.

Kinetic Studies of the Alteration of b_{561} at pH 8.0. A 500 μL sample of purified, $K_3Fe(CN)_6$-oxidized b_{561} (17 μM) in storage buffer was diluted with 6.5 mL of 100 mM potassium phosphate buffer, pH 8.0, containing 20 mM tyramine, 20% (w/v) glycerol, 1% (w/v) *n*-octyl β-D-glucopyranoside. The mixture (total volume 7.0 mL) was incubated at 25 °C in a constant-temperature bath and, a 350 μL aliquot was withdrawn at the desired time and the spectrum recorded against a blank which was identical to the test incubate, except that b_{561} was replaced with the same volume of storage buffer. Then, the sample was reduced with 2 mM Asc followed by 5 mM sodium dithionite and spectra were recorded immediately after each step. The same procedure was repeated for all the other time points. The spectra of all the final dithionite-reduced samples were recorded again after 3 h. All spectra were corrected for dilution (final total volumes were 370 μL) and normalized to the initial (350 μL) volume, where appropriate (see the corresponding figure legends for further experimental details).

Reversibility of the pH-induced Alteration of Purified $b_{561,ox}$ Upon pH Readjustment. A 100 μL sample of $b_{561,ox}$ (~7.2 μM) in 200 μL of 100 mM potassium phosphate buffer, pH 8.0, containing 20% (w/v) glycerol, 1% (w/v) *n*-octyl β-D-glucopyranoside, and 100 μg/mL catalase was incubated at 25 °C for 2 h. After the incubation period, the sample was reduced with 2.0 mM Asc and the UV−vis spectrum was recorded. The pH of the Asc-reduced sample was adjusted to 6.5 with dilute HCl, incubated at 4 °C for 1 h, warmed to 25 °C and the spectrum was recorded. Finally, the sample was reduced with 5.0 mM dithionite and the spectrum was recorded. The pH-adjusted dithionite-reduced sample was concentrated to about 50 μL in a Microcon YM-30 ultrafiltration device and washed twice with 300 μL aliquots of 100 mM potassium phosphate buffer, pH 8.0, containing 20% (w/v) glycerol, 1% (w/v) *n*-octyl β-D-glucopyranoside, and 100 μg/mL catalase by ultrafiltration. The protein was reconstituted with the same buffer (total volume 300 μL) and completely oxidized with just enough $K_4Fe(CN)_6$, reduced with 2.0 mM Asc, followed by 5.0 mM dithionite. The corresponding UV−vis spectra were recorded after each step.

EPR Studies of Cytochrome b_{561}. Purified reduced b_{561} in 100 mM potassium phosphate buffer, pH 6.8, containing 1% (w/v) *n*-octyl β-D-glucopyranoside, 20% (w/v) glycerol was oxidized just to completion by adding aliquots of 20 mM $K_3Fe(CN)_6$. The extent of oxidation was monitored by diluting a small sample into deoxygenated buffer and measuring the UV−vis spectra. Immediately after complete oxidation, 25 μL samples were transferred to EPR tubes and frozen in liquid nitrogen and EPR spectra were subsequently recorded. When necessary, $K_3Fe(CN)_6$-oxidized samples were passed through a Superdex 200 gel filtration column (Pharmacia-LKB) preequilibrated with 50 mM potassium phosphate buffer, pH 7.0 (4 °C), containing 1% (w/v) *n*-octyl β-glucopyranoside and 0.5 M NaCl to remove the $K_4Fe(CN)_6$, $K_3Fe(CN)_6$, and other extraneous impurities. Repurified oxidized b_{561} samples were reconstituted into 100 mM potassium phosphate buffer, pH 8.0 (4 °C), containing 1% (w/v) *n*-octyl β-glucopyranoside and 20% (w/v) glycerol and concentrated by ultrafiltration in an Amicon cell using a YM 30 membrane. Samples of oxidized, repurified b_{561} (25 μL; 200 μM) were transferred to EPR tubes immediately after concentration and were frozen in liquid nitrogen for subsequent EPR studies. Concentration of the EPR samples were estimated spectroscopically using the extinction coefficient of 267.9 mM^{-1} cm^{-1} at 427 nm (*29*).

To examine the time-dependent alteration of oxidized b_{561}, the frozen samples were thawed and incubated for 1 h at 25 °C and was refrozen again in liquid nitrogen and the EPR spectra were recorded at 15 and 4 K using the same spectroscopic parameters listed in Materials and Methods. The same procedure was repeated for 2 and 3 h incubations. Finally, the b_{561} sample was reduced with Asc followed by dithionite and the corresponding EPR spectra were also recorded at 15 and 4 K. When necessary, samples were thawed and immediately made to contain 20 mM tyramine, incubated for 5 min at room temperature, frozen in liquid nitrogen, and the EPR spectra were recorded under the above conditions.

Data Analysis. All kinetic data were analyzed by nonlinear least-squares fit of the spectral data to the desired kinetic equations using Sigma Plot. The applicable kinetic schemes were determined based on the standard errors, residuals, as well as examining the deviation of the experimental data from the calculated curves.

RESULTS

Spectroscopic Characteristics of Purified b_{561}. The single column purification procedure detailed in Experimental Section yielded electrophoretically pure b_{561} in high yield (further details of this purification will be published elsewhere). As shown in Figure 1, both Asc and dithionite-reduced, purified b_{561} displayed the characteristic UV−vis spectra with a Soret band at 427 nm and α- and β-bands at 561 and 530 nm. However, the relative intensities of the 427

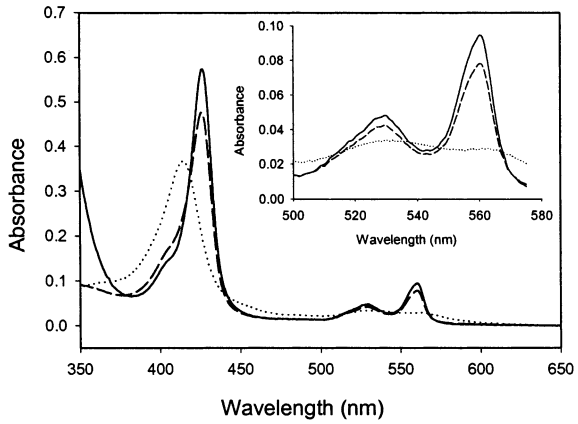

FIGURE 1: UV−vis spectra of oxidized and reduced b_{561}: dotted line, $K_3Fe(CN)_6$-oxidized b_{561}; dashed line, 2 mM Asc-reduced b_{561}; solid line, 5 mM dithionite-reduced b_{561}. All the spectra were recorded at 25 °C in 100 mM potassium phosphate buffer, pH 6.8, containing 20% (w/v) glycerol, 1% (w/v) *n*-octyl β-D-glucopyranoside.

nm absorption bands indicate that while most of the freshly isolated $K_3Fe(CN)_6$-oxidized b_{561} can be reduced by Asc (2 mM) the remaining can only be reduced by dithionite (5 mM) at pH 6.8. The A_{427}/A_{561} ratios for Asc- and dithionite-reduced b_{561} are 5.82 and 5.63, respectively, at pH 6.8. In addition, A_{427}/A_{415} ratios for Asc and dithionite-reduced b_{561} are 1.24 and 1.45, respectively, demonstrating that freshly isolated b_{561} contains ~85−90% Asc reducible and ~10−15% Asc nonreducible but dithionite reducible populations of b_{561}, at pH 6.8.

Alteration of $b_{561,ox}$ at pH 8.0. Incubation of $K_3Fe(CN)_6$-oxidized b_{561} ($b_{561,ox}$) at pH 8.0 and 25 °C resulted in a time-dependent shift of the Soret band at 415 nm (characteristic for native $b_{561,ox}$) to 410 nm and the appearance of a weak band in the 610 nm region. After 1 h incubation under the above conditions, only about 50% of the protein could be reduced to the native form with 2 mM Asc. The remaining Asc nonreducible portion showed an absorption band at about 408 nm as a shoulder. Further reduction of the Asc-reduced sample with 5 mM dithionite in the presence of atmospheric oxygen almost completely removed the band at 408 nm, but only about 10−15% of the intensity of the 561 nm absorption band was increased. When similar experiments were carried out in the presence of 20 mM DA, E, NE, or tyramine the above shifts were more pronounced and the intensity of the 610 nm band was significantly higher. Therefore, all the detailed and quantitative studies were carried out in the presence of 20 mM tyramine.

As shown from the spectra in Figure 2, incubation of the purified $b_{561,ox}$ at pH 8.0 and 25 °C in the presence of 20 mM tyramine altered its characteristic UV−vis spectrum in a time-dependent manner. The Soret band at 415 nm gradually shifted to a new less intense band at 407 nm with a well-defined isobestic point at 404 nm (Figure 2A). In addition, both the α- and β-bands decayed slowly, and two new absorption bands appeared at 610 and 495 nm regions in a time-dependent manner (Figure 2B). The rates of these changes significantly increased with increasing pH and temperature (see below), but were not significantly affected by the absence of tyramine. The control experiments revealed that the spectrum of altered b_{561} is distinctly different from the spectrum of free heme in the same solution (data not

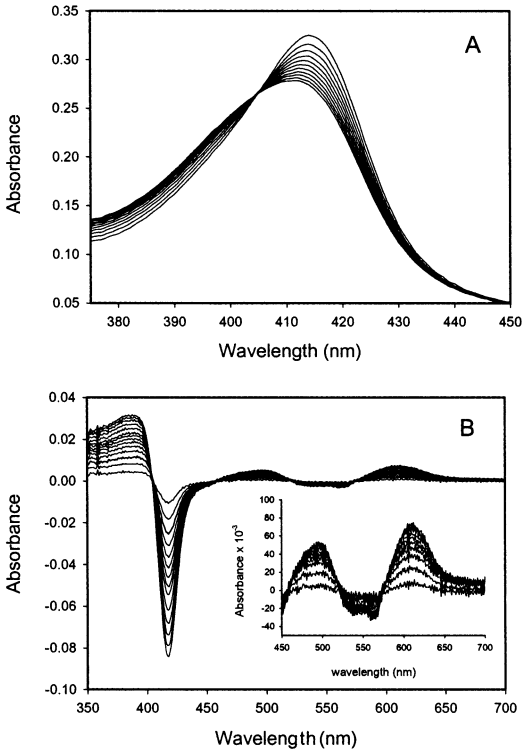

FIGURE 2: Time course of UV−vis spectral alteration of $b_{561,ox}$ at pH 8.0 and 25 °C: (A) $K_3Fe(CN)_6$-oxidized b_{561} was incubated at 25 °C in 100 mM potassium phosphate buffer, pH 8.0, containing 20% (w/v) glycerol, 1% (w/v) *n*-octyl β-D-glucopyranoside, and 20 mM tyramine, and the UV−vis spectra were recorded every 3 min for a period of 66 min. (B) Difference spectra derived from the data in panel A by mathematically subtracting the spectra from the time zero spectrum.

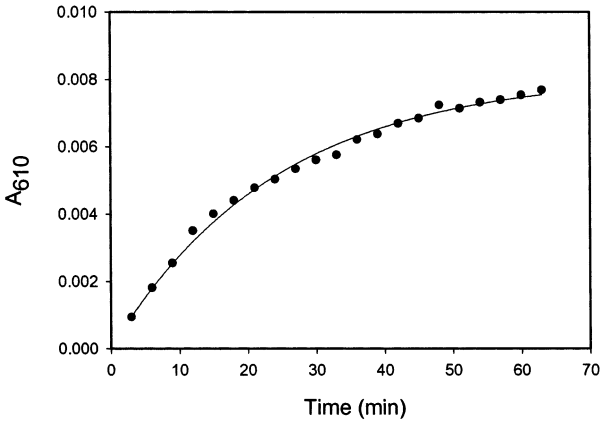

FIGURE 3: Kinetics of the increase in intensity of the absorption band at 610 nm during the incubation of $b_{561,ox}$ at pH 8.0 and 25 °C: (●) A_{610}; solid line, Theoretical fit of the experimental data to the first-order growth equation $A_t = A_0(1 - e^{-kt})$. The experimental conditions are identical to those in Figure 2.

shown). In contrast to the behavior of $b_{561,ox}$, the reduced form did not display any spectral alterations under similar conditions even with longer periods of incubation. As shown in Figure 3, the alteration of the $b_{561,ox}$ under the above experimental conditions could be quantified by the time-dependent increase of the intensity of the well-resolved absorption band at 610 nm. The direct fit of the increase in A_{610} with time to the first-order growth equation $A_t = A_0(1 - e^{-kt})$ yielded a first-order rate constant of $(4.13 \pm 0.15) \times 10^{-2}$ min^{-1}. Furthermore, the data could

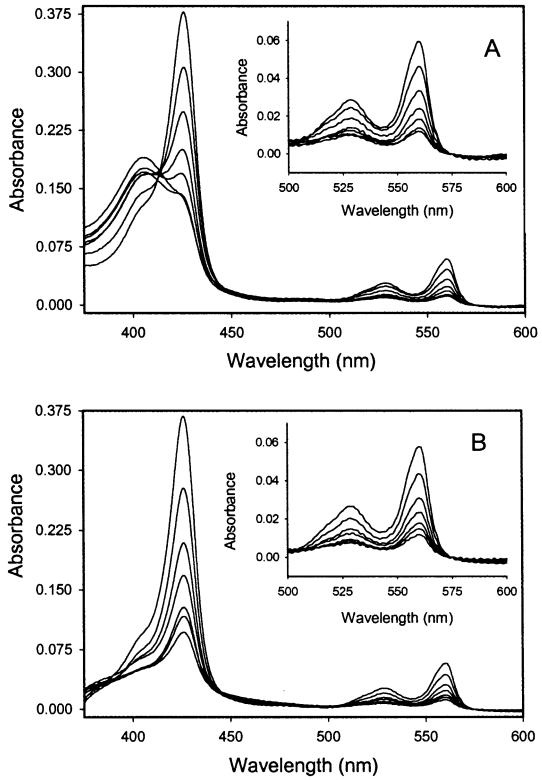

FIGURE 4: Reduction of mild alkaline treated $b_{561,ox}$ with Asc and dithionite: A solution of 1.1 μM $b_{561,ox}$ in 100 mM potassium phosphate buffer, pH 8.0, containing 20% (w/v) glycerol, 1% (w/v) *n*-octyl β-D-glucopyranoside in a total volume of 7.0 mL was incubated at 25 °C. At each 10−12 min time interval, 350 μL aliquots of the incubate were withdrawn and reduced with 2 mM Asc followed by 5 mM dithionite and the spectra were recorded immediately (A) 2 mM Asc-reduced spectra; inset: expanded 500−600 nm region; (B) 5 mM dithionite-reduced spectra; inset: expanded 500−600 nm region. Only every ~30 min time traces are shown to improve the clarity.

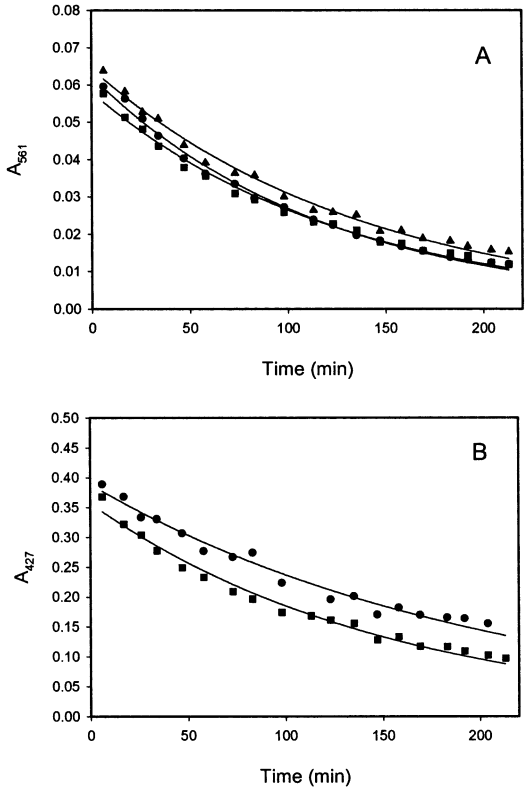

FIGURE 5: Kinetics of the Transformation of the Native $b_{561,ox}$ to Asc Nonreducible Altered Form: A 1.2 μM solution of $b_{561,ox}$ in 100 mM potassium phosphate buffer, pH 8.0, containing 20% (w/v) glycerol, 1% (w/v) *n*-octyl β-D-glucopyranoside in a total volume of 7.0 mL was incubated at 25 °C. At each ~10 min time interval, 350 μL aliquots of the incubate were withdrawn and reduced with 2 mM Asc followed by 5 mM dithionite and the spectra were recorded immediately. The time course of the transformation of the native $b_{561,ox}$ to altered Asc nonreducible form, (A) as determined by the decay of the 561 nm band of 2 mM Asc- and 5 mM dithionite-reduced spectra; (▲) immediately after Asc addition; (●) immediately after dithionite addition; (■) at the end of the experiment; (B) as determined by the decay of the 427 nm band of 5 mM dithionite-reduced spectra as a function of time (●) immediately after dithionite addition; (■) at the end of the experiment. Solid curves represent the fit of the experimental data to the unimolecular decay equation $A_t = A_0e^{-kt}$.

not be satisfactorily fitted to any other kinetic process including a double exponential decay (Figure 3).

Characteristics of the Altered $b_{561,ox}$ at pH 8.0. The characteristics of the altered, $b_{561,ox}$ were further examined through a series of experiments. In these experiments, purified $b_{561,ox}$ was incubated at pH 8.0 and 25 °C and aliquots were withdrawn at fixed time intervals and reduced with 2 mM Asc followed by 5 mM dithionite (for further experimental details see the corresponding figure legends and Materials and Methods). The corresponding UV−vis spectra of each sample were recorded immediately after each step and 3 h after the addition of dithionite. The data presented in Figure 4A demonstrate that the amount of Asc reducible $b_{561,ox}$ gradually and continuously decreases with time, with the concomitant increase of the Asc nonreducible form with an absorption maximum at about 405 nm in the presence of 20 mM tyramine (408 nm in the absence of tyramine). Normally, 3 h incubation under the above conditions resulted in the conversion of more than 80% of the Asc reducible $b_{561,ox}$ to the Asc nonreducible altered form (Figure 4A). Further reduction of the Asc-reduced samples with sodium dithionite in the presence of atmospheric oxygen completely bleached the spectral bands corresponding to the altered form with only about 10−15% increase of the reduced b_{561} (similar to the native freshly isolated b_{561}) regardless of the incubation time (Figure 4A,B). The overlay of the α-and β-absorption band regions of Asc-reduced and Asc- followed by dithionite-reduced spectra clearly indicate that about 10−15% of Asc nonreducible heme is reduced to native b_{561} and the remainder is destroyed instantaneously by dithionite addition (data not shown).

Kinetics of pH-Dependent Alteration of $b_{561,ox}$. The data presented in Figure 4A,B indicate that the time course of the pH-dependent alteration of $b_{561,ox}$ to produce the Asc nonreducible form could conveniently be monitored by following the absorption band at 561 nm of the reduced protein with incubation time. As shown in Figure 5A, the decay of the 561 nm bands of both Asc- and dithionite-reduced incubates could be best fitted to a first-order exponential decay equation $A_t = A_0e^{-kt}$ for the entire period of incubation (0−230 min) but not to an equation with double exponentials. The data presented in Table 1 indicate that the rate constants for the decay of the 561 nm band of Asc- and dithionite-reduced samples are similar, again confirming that most of the Asc nonreducible altered form could not be reduced by dithionite either (similar results were also obtained in the absence of tyramine). In addition, further

Table 1: Rate Constants for the Alteration of $b_{561,Ox}$ to Asc Nonreducible Form at pH 8.0 and 25 °C[a]

	determined from A_{561}		determined from A_{427}	
reduced with	$k \times 10^{-2}$ min^{-1}	$A_{0,561} \times 10^{-2}$ [b]	$k \times 10^{-2}$ min^{-1}	$A_{0,427} \times 10^{-2}$ [b]
ascorbate[a]	0.84 ± 0.02	6.2 ± 0.2	[c]	[c]
dithionite[d]	0.73 ± 0.02	6.4 ± 0.2	0.50 ± 0.02	38.8 ± 0.7
dithionite[e]	0.79 ± 0.02	5.8 ± 0.1	0.66 ± 0.02	35.7 ± 0.6

[a] The first-order rate constant, (k) and absorbance at $t = 0$ ($A_{0,561}$ and $A_{0,427}$) were determined by fitting the 561 and 427 nm absorbance data of the Asc- and dithionite-reduced spectra of Figure 5 to $A_t = A_0 e^{-kt}$ as detailed in Materials and Methods and Results. [b] A_0 is in absorbance units. These values are reported for comparison purposes and to show the internal consistency of the experimental data. [c] The absorbance at 427 nm could not be accurately determined due to the overlap of the 427 nm absorption band with the altered heme spectrum of Asc-reduced spectra (see Figure 4A). [d] The kinetic parameters were obtained from the spectra recorded immediately after dithionite reduction. [e] The kinetic parameters obtained from the spectra recorded 3 h after dithionite reduction.

incubation of the final dithionite-reduced samples does not significantly affect the intensity of the 561 nm band or the rate constant of the decay, confirming that only the oxidized protein is susceptible to the pH-induced alteration. The decay of the 427 nm absorption band of Asc-reduced samples could not be quantified accurately due to the presence of an overlapping absorption band of the altered protein. However, since overlapping bands are bleached by dithionite, the rate of decay of the 427 nm band could be determined by following its intensity in dithionite-reduced samples. Again, similar to the behavior of the 561 nm band, the decay of the 427 nm band could only be fitted to a single exponential decay equation (Figure 5B). The data presented in Table 1 demonstrate that the magnitudes of the rate constants for the decay of the 427 nm band of the dithionite-reduced samples are in the same range as for the 561 nm bands of both Asc- and dithionite-reduced samples (Table 1; slightly smaller magnitudes of the rate constants could be due to the high background absorbance at 427 nm).

Reversibility of pH Altered $b_{561,ox}$. Incubation of $b_{561,ox}$ at pH 8.0 and 25 °C for 2 h converts about 60% of the native $b_{561,ox}$ to the Asc nonreducible altered form, as expected (Figure 6A, dashed line). The pH adjustment of the sample to 6.5 followed by incubation at 4 °C for 1 h did not increase the amount of reduced b_{561} significantly, but shifted the 405 nm absorption band which corresponds to the altered protein, to 412 nm (Figure 6A; dotted line). Interestingly, the reduction of the pH adjusted sample with 5.0 mM dithionite did not bleach the heme spectrum as in the case of pH unadjusted samples, but shifted the Soret band from 412 to 426 nm giving a spectrum that is similar to that of the native reduced b_{561} (Figure 6A; solid line). Quantification of the dithionite-reduced protein, based on the intensity of the 561 nm band, revealed that more than 50% of the altered b_{561} is converted back to the native form by the pH adjustment followed by dithionite reduction (total recovery is about 70% of the original). The pH adjusted, dithionite-reduced protein was further characterized after removing excess Asc, dithionite, and other reagents by ultrafiltration. As shown in Figure 6B (dashed line), while ~85% of the ultrafiltered $K_4Fe(CN)_6$-oxidized b_{561} was Asc (2 mM) reducible, the remainder was dithionite (5 mM) reducible (Figure 6B, solid line) similar to native b_{561}, suggesting that pH-adjusted and dithionite-reduced protein behaves similar to native b_{561}.

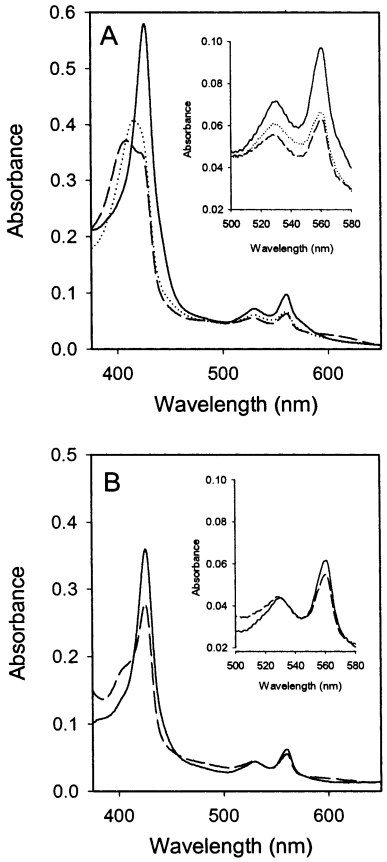

FIGURE 6: Reversibility of the pH-induced alteration of $b_{561,ox}$ upon pH readjustment: A 2.4 μM solution of $b_{561,ox}$ was incubated in 100 mM potassium phosphate buffer, pH 8.0, containing 20% (w/v) glycerol, 1% (w/v) *n*-octyl β-D-glucopyranoside, 100 μg/mL catalase at 25 °C for 2 h and reduced with 2.0 mM Asc. The pH of the sample was adjusted to 6.5, and further incubated for 1 h at 4 °C. After the incubation, the sample was reduced with 5.0 mM dithionite and ultrafiltered using a Microcon YM-30 ultrafiltration device. The retentate was reconstituted with the above buffer, oxidized with $K_4Fe(CN)_6$, and reduced with 2.0 mM Asc, followed by 5.0 mM dithionite. After each step the UV−vis spectra of the samples were recorded. Panel A: (a) dashed line, the spectrum of $b_{561,ox}$ after 2 h incubation, followed by Asc reduction; (b) dotted line, (a) after the pH adjustment; (c) solid line, (b) after the dithionite reduction. Panel B: (d) dashed line, (c) after ultrafilteration, $K_4Fe(CN)_6$ oxidation, followed by 2.0 mM Asc reduction; solid line, (d) after the dithionite reduction.

EPR Studies. The low temperature (15 K) EPR spectra shown in Figure 7A clearly indicate that freshly isolated $b_{561,ox}$ contains very low levels of high spin heme at pH 8.0 (EPR signal at $g = 6.0$ and $g = 2.0$). While the strong low spin heme signal at $g_x = 3.14$, $g_y = 2.10$, and $g_z = 1.49$ dominate the spectrum, there is also a signal with very low intensity at 3.7 and a second at 4.3. Incubation of oxidized $b_{561,ox}$ at 25 °C and pH 8.0 converts the low spin signal at $g_x = 3.14$, $g_y = 2.10$, and $g_z = 1.49$ to a typical high spin signal at $g_\perp = 6.0$ and $g_\parallel = 2.0$ in a time-dependent manner (Figure 7). Interestingly, in the presence of 20 mM tyramine (not optimized), the high spin signal splits into three very distinct peaks, suggesting a strong interaction of tyramine with the altered high spin heme of $b_{561,ox}$ (Figure 7B,C).

The EPR spectra shown in Figure 8B,C, which were recorded after the gel-filtration of the $K_3Fe(CN)_6$-oxidized

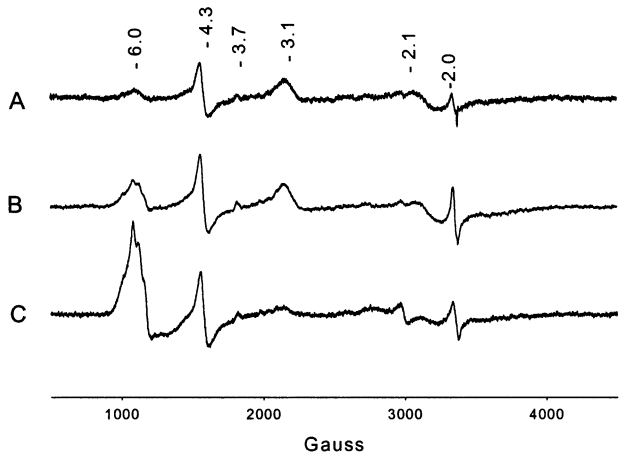

FIGURE 7: Effect of tyramine on the EPR spectra of altered $b_{561,ox}$: All the EPR spectra were recorded at 15 K at 9.46 GHz using 20.0 mW power, modulation frequency 100 kHz, and modulation amplitude of 10 G. The sample contained 150 μM $K_3Fe(CN)_6$-oxidized b_{561} in 100 mM potassium phosphate buffer, pH 8.0, containing 20% (w/v) glycerol, 1% (w/v) *n*-octyl β-D-glucopyranoside. (A) immediately after oxidation; (B) A in the presence of 20 mM tyramine; (C) B after 3 h incubation.

FIGURE 8: Effect of Gel filtration on the EPR Spectra of $b_{561,ox}$. All the EPR spectra were recorded under the same conditions as in Figure 7, except that $K_3Fe(CN)_6$-oxidized b_{561} (Figure 7A) was further purified by gel filtration as described in Experimental Section at pH 7.0. The repurified sample was reconstituted into 100 mM potassium phosphate buffer, pH 8.0, containing 20% (w/v) glycerol, 1% (w/v) *n*-octyl β-D-glucopyranoside, and concentrated (200 μM). The concentrated sample was transferred into an EPR tube and frozen immediately in liquid nitrogen. (A) Immediately after oxidation (same as Figure 7A; included for comparison purposes); (B) A after gel-filtration followed by reconstitution to pH 8.0; (C) B after 2 h incubation at 25 °C; (D) C after reduction with 2 mM Asc.

protein [$b_{561,ox}$; to remove the excess $K_3Fe(CN)_6$, $K_4Fe(CN)_6$, and other impurities), show that both 3.7 and 4.3 EPR signals were absent in these repurified samples. Comparison of the EPR spectra in Figure 8, panel A with B indicates that the manipulation of the oxidized protein i.e., gel-filtration (at pH 7.0) followed by concentration (at pH 8.0, 4 °C), increased the high spin heme signal at $g_\perp = 6.0$ and $g_\parallel = 2.0$ significantly. In addition, further incubation of these EPR samples at 25 °C and pH 8.0 increased the intensity of the high spin signal with the concomitant decrease of the intensity of the low spin signal at 3.14 (Figure 8B,C) as seen with non-gel-filtered $b_{561,ox}$ samples. During the 2 h incubation period, most of the low spin $g_x = 3.1$, $g_y = 2.1$, and $g_z = 1.49$ EPR signal converted to the high spin signal at $g_\perp = 6.0$ and $g_\parallel = 2.0$ (Figure 8C). The EPR spectrum in Figure 8D shows that while the remaining low spin heme in 2 h incubated EPR sample is reduced, some of the high spin heme is not reduced by Asc. However, Asc reduction causes significant sharpening of the high spin signal. In addition, the $g_\parallel = 2.0$ component of the high spin heme signal is clearly visible in the Asc-reduced spectrum (Figure 8C). On the other hand, dithionite completely removes the Asc nonreducible heme signals in the sample (data not shown).

DISCUSSION

The above results clearly show that purified $b_{561,ox}$ readily transforms into an altered high spin form in a pH- and time-dependent manner as indicated by the characteristic changes of the UV−vis (Figures 2 and 3) and EPR (Figure 8) spectra. The quantitative analysis of this transformation by monitoring the increase in intensity of the characteristic high spin heme absorption band at 610 nm (*39*−*40*), as a function of time, demonstrate that it is a well-behaved apparent unimolecular process with a rate constant of 4.1 ± 0.2 min^{-1} at pH 8.0 and 25 °C in the presence of 20 mM tyramine (Table 1).[2]

The characteristics of the altered $b_{561,ox}$ are intriguing. While some of the altered high spin form of $b_{561,ox}$ (see below) could not be reduced with Asc, attempted reduction with dithionite completely bleached the Asc nonreducible portion of the heme spectrum (Figure 2). Control experiments revealed that the transformation of the $b_{561,ox}$ to the Asc nonreducible form is also time dependent and could be followed by monitoring the decay of the 561 nm absorption band of Asc- and dithionite-reduced (Figure 4A,B) or 427 nm band of dithionite-reduced (Figure 4B) samples. The kinetic studies demonstrate that the conversion of $b_{561,ox}$ to the Asc nonreducible form is also an apparent unimolecular process (Figure 5A,B) which could be described by a single-exponential decay (both in the presence and absence of tyramine) regardless of whether the 561 or 427 nm bands were monitored. The apparent first-order rate constants determined for the decay of these bands for Asc- or dithionite-reduced samples were similar[3] confirming that most of the Asc nonreducible $b_{561,ox}$ could not be reduced with dithionite either, to give the native protein (Table 1).

[2] In the absence of tyramine, the intensity of the 610 nm absorption band is relatively small; thus, accurate kinetic parameters could not be determined.

[3] Tyramine does not significantly affect the rate of irreversible transformation of b_{561}.

Scheme 1

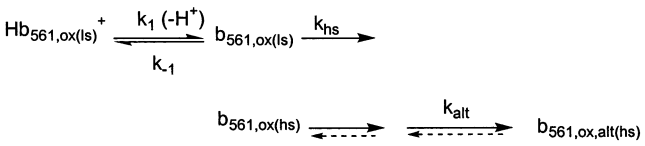

The rate constants for the initial conversion of native low spin $b_{561,ox}$ to the high spin form is about 6 times faster than that of the alteration to the Asc nonreducible form under the same experimental conditions, suggesting that the initially produced high spin form is further transformed to an Asc nonreducible from, in a kinetically slower second step. The presence of a strong high spin EPR signal at $g_\perp = 6.0$ and $g_{||} = 2.0$ (Figure 8D) and 610 nm band in UV−vis spectra of Asc-reduced, incubated samples clearly indicate that the Asc nonreducible protein is also a high spin species. The observed significant sharpening of the high spin EPR signal upon Asc reduction of the incubated samples (Figure 8C,D) suggest that they may contain a mixture of high spin heme species and reduction with Asc regenerates the native b_{561} only from a fraction of the altered protein under the experimental conditions.

On the basis of the above observations, the following minimal kinetic scheme is proposed for the pH-dependent alteration of $b_{561,ox}$ (Scheme 1). In the scheme, $Hb_{561,ox(ls)}^{+}$, $b_{561,ox(ls)}$, $b_{561,ox,(hs)}$, and $b_{561,ox,alt(hs)}$ are native protonated, native unprotonated, unprotonated high spin, and altered unprotonated high spin forms of $b_{561,ox}$, respectively. In addition, except $b_{561,ox,alt(hs)}$, all the other forms of $b_{561,ox}$ are reducible to the native b_{561} by Asc and they are indistinguishable from each other in the reduced state. As mentioned above, the conversion of the native $b_{561,ox}$ to the high spin species, $b_{561,ox(hs)}$, is an apparent first-order process, suggesting that the deprotonated and protonated forms of native $b_{561,ox}$ are in rapid equilibrium or the deprotonation is a kinetically relatively rapid process with $k_{hs} \ll k_{-1}$ under the experimental conditions. Under these conditions, the apparent first-order rate constant for the formation of the high spin species must be a function of $[H^+]$ which is in agreement with the experimental observations. In addition, as mentioned above, the conversion of the $b_{561,ox}$ to its Asc nonreducible form is also an apparent first-order process, suggesting that k_{alt} must be relatively smaller than the other rate constants and must be rate limiting under the experimental conditions. This conclusion is also in agreement with the finding that the magnitude of the apparent first-order rate constant for the formation of high spin species is about 5−6 times greater than that of the formation of the Asc nonreducible form at pH 8.0. Finally, the pH readjustment to 6.5 followed by dithionite reduction causes the reversal of the alteration process to regenerate the native protein, at least partially.

Previous studies (*29*−*32*, *34*) have reported that while two chemically distinct heme centers are present in purified b_{561}, one heme center of the oxidized protein is labile and loses the ability to accept electrons from Asc upon mild alkaline treatment (pH 8.0). However, the above kinetic studies indicate that the mild alkaline-mediated alteration of the native $b_{561,ox}$ to the initial high spin form or to the final Asc nonreducible form **does not** terminate at 50% conversion. In fact, within the experimental time frame (210 min), while almost all the heme was converted to the initial high spin form, ~85% was converted to the Asc nonreducible form at pH 8.0 and 25 °C (Figures 3 and 5). In addition, the kinetics of both these transformations could be best described by rate equations with single exponentials and two parameters (i.e., $A_t = A_o(1 - e^{-kt})$ and $A_t = A_o e^{-kt}$, respectively; Figures 3 and 5 and Table 1). Although, one can argue that the unimolecular decay kinetics observed in this study may reflect the pH-dependent irreversible unfolding and/or denaturing of the protein, the observed reversibility of the alteration of $b_{561,ox}$ strongly argue against such a possibility. The recovery of more than 50% of the Asc nonreducible $b_{561,ox,alt}$, in the native form after the pH adjustment followed by reduction with dithionite (Figure 6), clearly demonstrate that most of the Asc nonreducible protein is **not** irreversibly denatured. Therefore, the observed alteration of $b_{561,ox}$ could well be a localized reversible alteration of the heme environment of the protein. Thus, the observed unimolecular decay kinetics could only be explained by assuming that both heme centers (if two heme centers are present in purified $b_{561,ox}$) undergo pH-dependent alterations with similar kinetics.

The observation of a typical low spin heme signal at $g_x = 3.14$, $g_y = 2.10$, and $g_z = 1.49$[4] and a highly anisotropic low spin signal at 3.7 in low-temperature EPR spectra of $b_{561,ox}$ has led to the proposal that two chemically inequivalent heme centers are present in the purified protein (*29*). On the basis of its high sensitivity to pH, the heme center corresponding to the signal at $g_x = 3.14$, $g_y = 2.10$ and $g_z = 1.49$ has been assigned as alkaline labile (*29*). Our low temperature EPR studies with highly purified b_{561} under similar experimental conditions also show that the low spin heme center with the EPR signal at $g_x = 3.14$, $g_y = 2.10$, and $g_z = 1.49$ is sensitive to pH [in agreement with the ref *29*],[4] and is converted to a typical high spin species with an EPR signal at $g_\perp = 6.0$ and $g_{||} = 2.0$ at pH 8.0 and 25 °C[5] in a time-dependent manner (Figure 7).[6] However, the behaviors of the EPR signal at $g = 3.7$ in our b_{561} preparations were noticeably different from those previously reported. For example, (a) the intensity of this signal in our $b_{561,ox}$ preparations is much smaller (Figure 7) and does not change

[4] This signal was shown to interchange with a second low spin EPR signal at $g_z = 2.84$, $g_y = 2.24$, and $g_x = 1.66$ (ref *29*). However, we have not observed this signal consistently. For example, while the spectra in Figure 7 show no indication of this signal, spectra B and C in Figure 8 show a very weak signal at $g = 2.96$. Since this signal is shown to be a temperature- and pH-dependent variant of the signal at $g_x = 3.14$, $g_y = 2.10$, and $g_z = 1.49$ (*29*), differences in experimental conditions may have led to the weakening of this signal in our studies.

[5] In addition to the typical high spin signal at $g_\perp = 6.0$ and $g_{||} = 2.0$, a signal at 2.2 is also increased with incubation time which is remarkably similar to the g_y component of the alkaline-treated purified b_{558} (g_z =2.42, $g_y = 2.23$, and $g_x = 1.91$) which is assigned as thiolate or hydroxide coordinated low spin heme similar to P_{450} [Fujii, H., Johnson, M. K., Finnegan, M. G., Miki, T., Yoshida, L. S., Kakinuma, K. (1995) *J. Biol. Chem. 270*, 12685−12689]. However, the lack of a parallel increase of the intensity of $g_z = 2.42$ (especially in Figure 7C) and the fact that this species is reducible with Asc argue against a similar assignment. On the other hand, this could be associated with one of the high spin heme species. However, the magnitude appears to be somewhat higher than that of the usual $g_{||} = 2.0$ of high spin heme. Therefore, the origin of this signal remains uncertain at present. More spectroscopic studies are underway to fully assign the signals in this region.

[6] We did not attempt to quantitatively correlate the decay of the low spin signal $g_z = 3.14$, $g_y = 2.1$, and $g_x = 1.49$ with the growth of $g_\perp = 6.0$ and $g_{||} = 2.0$, since accurate quantification of nonsymmetrical and/or overlapping multiple signals by double integration may not be accurate.

with the temperature or pH [between temperatures 25 and 4 °K and pH values 4.5−8.5 (data not shown)] as previously reported (*29*); (b) gel-filtration of the $K_3Fe(CN)_6$-oxidized b_{561} completely removes both 3.7 as well as 4.3 EPR signals (Figure 8) but, does not alter the characteristic UV−vis spectrum of the protein; (c) gel-filtered samples display pH alteration kinetic parameters that were similar to non-gel-filtered samples, suggesting that the loss of 3.7 and 4.3 signals has no significant effect on the pH-induced alteration of the protein (data not shown); (d) although the intensity of this signal in the non-gel-filtered samples does not change during incubation at pH 8.0 and 25 °C, only 10−15% of Asc or dithionite reducible heme (by UV−vis) is present after the 3 h incubation period (Figure 7); (e) the heme center responsible for this signal is unlikely to be lost during the purification and/or gel-filtration process since A_{427}/A_{280} ratio for the gel-filtered EPR sample was similar to that reported in ref *29* (i.e., 3.7 and 3.9, respectively). Therefore, in contrast to the previous proposals (*27*−*29*, *33*), the origin or the significance of the EPR signal at 3.7 in purified $b_{561,ox}$ is not clear, at least in our hands. These uncertainties and the observed kinetics of the pH-dependent alteration of purified $b_{561,ox}$, as discussed above, raise some serious questions regarding the proposed two heme structural model of purified b_{561}. Certainly, further studies are necessary to fully explain these inconsistencies.

Ample spectroscopic and other evidence suggest that the heme in b_{561} is bis-histidine coordinated (*29*−*32*, *34*−*36*). Therefore, the slow conversion of the heme center(s) from low spin to high spin in the oxidized state under mildly alkaline conditions is likely to be due to the pH-dependent replacement of one of the axial histidines with a weak ligand such as water. Further strong evidence for the presence of a weak ligand in one of the axial positions of the heme center in altered b_{561} is derived from the observation that tyramine causes the splitting of the high spin EPR signal into three very distinct peaks (Figure 7B,C). We believe a strong interaction of tyramine with the high spin heme center of altered $b_{561,ox}$ causes the observed splitting of the EPR signal ($g = 6.27$, 5.98, and 5.72) as a consequence of the loss of axial symmetry of the heme plane due to the rhombic distortion (*41*) introduced by the interaction of tyramine. These findings together with the facts that spectral and the chemical properties of the altered Asc nonreducible protein are distinctly different from the free heme in solution, strongly suggest that the heme of altered $b_{561,ox}$ is protein bound most probably through the second axial histidine. This proposal is also substantiated by the reversibility of the alteration of $b_{561,ox}$ upon pH adjustment followed by the dithionite reduction and by the UV−vis and EPR spectral similarities between the altered $b_{561,ox}$ with other mono-histidine coordinated proteins such as hemoglobin and myoglobin (see below).

The rapid and complete bleaching of the heme spectrum of the altered Asc nonreducible $b_{561,ox}$ in the presence of dithionite is unexpected. Although rapid degradation of heme in Fe (III) hemoglobin and some other hemoproteins by H_2O_2 have been reported (*42*−*43*), dithionite-mediated complete destruction of the heme of hemoproteins is not common. However, complete bleaching of the erythrocyte unstable green hemoprotein (a variant of hemoglobin) by dithionite under aerobic conditions has been reported (*44*). In this case, the bleaching of the heme spectrum is attributed to the H_2O_2 and related radical species produced by dithionite under aerobic conditions. Therefore, since all the above experiments were carried out in the presence of atmospheric oxygen, the bleaching of the heme spectrum of altered, Asc nonreducible $b_{561,ox}$ in the presence of dithionite must also be associated with the production of H_2O_2 and other activated oxygen species. This notion is further supported by the finding that under anaerobic conditions or in the presence of catalase only a small amount of heme was lost under similar experimental conditions (unpublished results). Furthermore, the similar behavior of the pH altered Asc nonreducible $b_{561,ox}$ to erythrocyte unstable green hemoprotein with respect to dithionite-mediated bleaching of the heme spectrum further suggests that the altered $b_{561,ox}$ is also monohistidine coordinated.

Oxidative stress and/or free radical formation in the central and peripheral nervous system play a significant role in a number of neurodegenerative disorders and aging (*45*−*47*). Easily autooxidizable catecholamines, DA, NE, and E, are known to generate reactive organic radicals, H_2O_2, and reactive oxygen radicals due to their inherent redox properties under aerobic conditions (*48*−*49*). Therefore, catecholaminergic neurons are inherently subjected to high oxidative stress and to free radical damage in comparison to other types of neurons (*50*−*51*). Although most of the radical species are effectively scavenged by enzymatic defense mechanisms such as superoxide dismutase and catalase and by cellular antioxidants such as vitamin E, vitamin C, uric acid, and glutathione under in vivo conditions, their excessive generation may lead to extensive cellular damage (*52*−*54*).

The presence of high concentrations of Asc (20 mM) and an intricate b_{561}-mediated Asc regenerating mechanism together with the absence of antioxidants such as glutathione in catecholamine storage vesicles suggest that, in addition to providing reducing equivalents for the DβM monooxygenation reaction, Asc must also play a key role in the protection of catecholaminergic neurons from catecholamine-induced free radical damage. Therefore, the proper functioning of b_{561} may also be vital for relieving the high oxidative stress in catecholaminergic neurons. Since b_{561}-mediated Asc regeneration is energized by a high pH gradient across the granule membrane (interior pH 5.4 and exterior pH 7.4), which is generated and maintained by granule membrane proton translocating ATPase, the coordinated function of these two proteins are mandatory to maintain high levels of reduced Asc inside the granule. Consequently, the vesicular monoamine transporter mediated active uptake of catecholamines into secretory vesicles may also play an indirect but important role in protecting the cytosolic catecholamines from auto-oxidation. Therefore, malfunctioning of any of these proteins could lead to the increase of oxidative stress in catecholaminergic neurons. As shown above, mild oxidative stress and/or the dissipation of the pH gradient could trigger the alteration of $b_{561,ox}$ (if operative in vivo), excessive auto-oxidation of catecholamines, and excessive production of H_2O_2, eventually leading to the irreversible destruction of the heme in b_{561} resulting in a considerable amplification of oxidative stress in these neurons. Therefore, the above findings may provide an additional basis for the high susceptibility of catecholaminergic neurons to oxidative stress. Further studies for the characterization of the molec-

ular details of the pH-induced alteration of $b_{561,ox}$ with respect to the proposed models and its extreme susceptibility toward oxidative degradation of heme are currently in progress.

ACKNOWLEDGMENT

We wish to thank Dr. Mike Gangel (USDA) for his aid in obtaining fresh adrenal glands for the isolation of b_{561}.

REFERENCES

1. Ingebretsen, O. C., Terland, O., and Flatmark, T. (1980) *Biochim. Biophys. Acta 628*, 182−189.
2. Phillips, J. H. (1982) *Neuroscience 7*, 1595−1609.
3. Diliberto E. J., Jr., and Allen, P. L. (1980) *Mol. Pharmacol. 17*, 421−426.
4. Diliberto E. J., Jr., and Allen, P. L. (1981) *J. Biol. Chem. 256*, 3385−3393.
5. Skotland, T., and Ljones, T (1980) *Biochim. Biophys. Acta 630*, 30−35.
6. Dhariwal, K. R., Black, C. D., and Levine, M. (1991) *J. Biol. Chem. 266*, 2908−12914.
7. May, J. M. (1998) *Front. Biosci. 3*, D1-D10
8. Foyer, C. H., and Halliwell, B. (1977) *Phytochemistry 61*, 1347−1350.
9. Mapson, L. W., and Moustafa, E. M. (1956) *Biochem. J. 62*, 248−259.
10. Tirrell, J. G., and Westhead, E. W. (1979) *Neuroscience 4*, 181−186.
11. Menniti, F. S., Knoth, J., and Diliberto, E. J., Jr. (1986) *J. Biol. Chem. 261*, 16901−16908.
12. Levine, M., Morita, K., Heldman, E., and Pollard, H. B. (1985) *J. Biol. Chem. 260*, 15598−15603.
13. Huyghe, B. G., and Klinman, J. P. (1991) *J. Biol. Chem. 266*, 11544−11550.
14. Levine, M., and Pollard, H. B. (1983) *FEBS Lett. 158*, 134−138.
15. Njus, D., and Kelly, P. M. (1993) *Biochim. Biophys. Acta 1144*, 235−248.
16. Njus, D., Knoth, J., Cook, C., and Kelley, D. M. (1983) *J. Biol. Chem. 258*, 27−30.
17. Kelley, D. M., and Njus, D. (1986) *J. Biol. Chem. 261*, 6429−6432.
18. Wakefield, L. M., Cass, A. E. G., and Radda, G. K. (1986) *J. Biol. Chem. 261*, 9739−9745.
19. Beers, M. F., Johnson, R. G., and Scarpa, A. (1986) *J. Biol. Chem. 261*, 2529−2535.
20. Wimalasena, K., and Wimalasena, D. S. (1995) *J. Biol. Chem. 270*, 27516−27524.
21. Apps, D. K., Pryde, J. G., and Phillips, J. H. (1980) *Neuroscience 5*, 2278−2287.
22. Perin, M. S., Fried, V. A., Slaughter, C. A., and Sudhof, T. C. (1988) *EMBO J. 7*, 2697−2703.
23. Kent, U. M., and Fleming, P. J. (1990) *J. Biol. Chem. 265*, 16422−16427.
24. Duong, L. T., and Fleming, P. J. (1982) *J. Biol. Chem. 257*, 8561−8564.
25. Apps, D. K., Boisclair, M. D., Gavine, F. S., and Pettigrew, G. W. (1984) *Biochim. Biophys. Acta 774*, 8−16.
26. Sisland, T., and Flatmark, T. (1974) *Biochim. Biophys. Acta 395*, 257−266.
27. Burbaev, D. Sh., Motoz, I. A., Kamenskiy, Yu. A., and Konstantinov, A. A. (1991) *FEBS Lett. 283*, 97−99.
28. Esposti, D. M., Kamenskiy, Y. A, Arutjunjan, A. M., and Konstantinov, A. A. (1989) *FEBS Lett. 254*, 74−78.
29. Tsubaki, M., Nakayama, M., Okuyama, E., and Ichikawa, Y. (1997) *J. Biol. Chem. 272*, 23206−23210.
30. Kobayashi, K., Tsubaki, M., and Tagawa, S. (1998) *J. Biol. Chem. 273*, 16038.
31. Okuyama, E., Yamamoto, R., Ichikawa, Y., and Tsubaki, M. (1998) *Biochim. Biophys. Acta 1383*, 269−278.
32. Tsubaki, M., Kobayashi, K., Ichise, T., Takeuchi, F., and Tagawa, S. (2000) *Biochemistry 39*, 3276−3284.
33. Kamensky, Y., A., and Palmer, G. (2001) *FEBS Lett. 491*, 119−122.
34. Takeuchi, F., Kobayashi, K., Tagawa, S., and Tsubaki, M. (2001) *Biochemistry 40*, 4067−4076.
35. Kipp, B. H., Kelley, P. M., and Njus, D. (2001) *Biochemistry 40*, 3931−3937.
36. Njus, D., Wigle, M., Kelley, P. M., Kipp, B. H., and Schlegel, H. B. (2001) *Biochemistry 40*, 11905−11911.
37. Kirshner, N. (1962) *J. Biol. Chem. 237*, 2311−2317.
38. Njus, D., and Radda, G. K. (1979) *Biochem. J. 180*, 579−585.
39. Barker, P. D., Nerou, E. P., Cheesman, M. R., Thomson, A. J., Oliveira, P. de, and Hill, A. O. (1996) *Biochemistry, 35*, 13618−13626.
40. Barker, P. D., and Freund, M. V. (1996) *Biochemistry, 35*, 13627−13635.
41. Peisach, J., Blumberg, W. E., Ogawa, S., Rachmilewitz, E. A., and Oltzik, R. (1971) *J. Biol. Chem. 246*, 3342−3355.
42. Nagabasu, E., and Rifkind, J. M. (1998) *Biochem. Biophys. Res. Commun. 247*, 592−596.
43. Nagabasu, E., and Rifkind, J. M. (2000) *Biochemistry 39*, 12503−12511.
44. DeFilippi, L. J., Ballou, D. P., and Hultquist, D. E. (1979) *J. Biol. Chem. 254*, 6917−6923.
45. Cadet, J. L., and Brannock, C. (1998) *Neurochem. Int. 32*, 117−131.
46. Jackson, G. R., Apfell, L., Werrbacch-Perez, K., and Perez-Polo, J. R. (1990) *J. Neurosci. Res. 25*, 360−369.
47. Ku, H.-H., Brunk, U. T., and Soghal, R. S. (1993) *Free Radical Biol. Med. 15*, 621−627.
48. Chance, B., Sies, H., and Boveris, H. (1979) *Physiol. Rev. 59*, 527−605.
49. Heikkila, R. E., and Mansino, L. (1987) *Ann. New York Acad. Sci. 498*, 63−76.
50. Cohen, G. (1987) *Adv. Neurol. 45*, 119−125.
51. Graham, D. G. (1978) *Mol. Pharmacol. 14*, 1819−1825.
52. Fridovich, I. (1983) *Annu. Rev. Pharmacol. 23*, 239−257.
53. Fridovich, I. (1986) *Arch. Biochem. Biophys. 247*, 1−11.
54. Frei, B., Englan, L., and Ames, B. N. (1989) *Proc. Natl. Acad. Sci. U.S.A. 86*, 6377−6381.

BI0206661